XAFS study of Mn-Ni/Al_2O_3 catalyst for carbon dioxide reforming of methane

Sun Hee Choi,[a*] Seung-Ho Seok[a] and Jae Sung Lee[a]

[a]*Department of Chemical Engineering/Research Center for Catalytic Technology, Pohang University of Science and Technology (POSTECH), San 31, Hyoja-dong, Nam-gu, Pohang 790-784, Republic of Korea. E-mail:shchoi@postech.ac.kr*

As an effective catalyst for carbon dioxide reforming of methane, manganese-promoted Ni/Al_2O_3 catalyst was studied with XAFS. The catalysts after the reduction above 1073 K contained the metallic nickel, and several phases of manganese were shown by XANES and EXAFS. Results of EXAFS curve fitting indicated that the surface of large metallic nickel particles was partly covered with patches of MnO and metallic Mn. Radial structure function (RSF) of Mn K-edge showed the peaks due to Mn-Ni scattering without Mn-Mn scattering, indicating that the metallic manganese was attached to nickel in a highly dispersed state. Separate manganese phase was also formed without interaction with nickel.

Keywords : XAFS, Mn-Ni/Al_2O_3 catalyst, carbon dioxide reforming of methane

1. Introduction

The catalytic reforming of methane with carbon dioxide into synthesis gas ($CO_2+CH_4 \rightarrow 2CO+2H_2$) is a desirable process since two greenhouse gases contributing to global warming can be converted to a valuable chemical feedstock. Coke formation via Boudouard reaction ($2CO \rightarrow C+CO_2$) and/or methane decomposition ($CH_4 \rightarrow C+2H_2$), has been a great obstacle in the industrial application despite a number of studies for this reaction. In general, noble metal catalysts are less sensitive to coke deposition than nickel-based catalysts. However, economic consideration makes it more desirable to develop an improved nickel-based catalyst that exhibits high coke resistance without sacrificing high activity.

Recently we have reported a remarkable additive effect of manganese on the performance of a nickel catalyst (Choi *et al.*, 1998; Seok *et al.*, 2000). In these studies, modified catalyst showed a drastic reduction in coke deposition with only a little lowering of catalytic activity. Among various modifiers such as Co, Cu, Zr, Mn, Mo, Ti, Ag, and Sn, Mn and Mo were found to be the most effective. In Mn-added Ni/Al_2O_3, the surface of nickel appeared to be partly covered by patches of MnO_x as evidenced by results of XRD, TEM and hydrogen chemisorption. Such a decoration should have assisted the suppression of coke deposition. As an extension of the previous works, we studied here manganese-promoted Ni/Al_2O_3 catalysts with X-ray Absorption Fine Structure (XAFS) spectroscopy. XAFS would reveal information on local atomic arrangement about each individual type of atoms as well as chemical properties such as coordination environment and the oxidation state.

2. Experimental and Data Analysis

Mn-promoted Ni/Al_2O_3 catalysts (molar ratio Ni:Mn:Al=1:1:6) were prepared by coprecipitation method using $Ni(NO_3)_2 \cdot 6H_2O$ (Aldrich), $Mn(NO_3)_2 \cdot 6H_2O$ (Aldrich), and γ-Al_2O_3 (Strem chemicals, BET surface area=164.1 m^2g^{-1}). As a reference, Ni-Al_2O_3 with 17 wt% Ni-metal loading was also prepared in a similar way.

Avoiding exposure to air, the catalysts calcined at 1123 K were pelletized into a self-supporting wafer and reduced at various temperatures in a controlled atmosphere XAFS cell (Lee *et al.*, 1996). XAFS measurements were performed on beamline 3C1 (monochromator crystal:Si(111); energy resolution $\Delta E/E = 2\times10^{-4}$; photon flux: 10^9-10^{10} photons·sec^{-1} in non-focused condition) of Pohang Accelerator Laboratory in Korea. Spectra at Ni and Mn K-edge were recorded in a transmission mode at room temperature. Two ionization chambers filled with nitrogen gases were used to measure the incident and the transmitted beam intensities.

The obtained XAFS data were analyzed by using UWXAFS 3.0 package (Stern *et al.*, 1995) and FEFF 8.0 code (Ankudinov *et al.*, 1998), both licensed from University of Washington. The normalization procedure has been previously reported in detail (Choi & Lee, 1997). The scaled EXAFS function $k^3\chi(k)$ of the momentum (k) space was converted to the R-space by Fourier transformation, resulting in the radial structural function (RSF) of the sample. With Fourier filtering, a shell of interest was inversely Fourier-transformed into a momentum space, and then, a nonlinear EXAFS fitting was performed.

3. Results and Discussion

The K-edge XANES spectra were adopted to probe the electronic state of Ni and Mn on Al_2O_3, as shown in Figure 1. The catalyst containing only nickel showed the same XANES feature as that of Ni foil, indicating that nickel in Ni/Al_2O_3 carried the metallic character. The addition of manganese did not affect this oxidation state of nickel except for Mn-Ni/Al_2O_3 reduced at 973 K which showed the feature of nickel oxide. Thus, reduction above 1073 K was needed to reduce completely the nickel in Mn-Ni/Al_2O_3 into the metallic state. The Mn K-edge XANES (Figure 1B) was a little more complicated. All manganese-added nickel catalysts showed pre-edge peak which was absent in Mn foil. However, the fine structures in the vicinity of the edge showed considerable differences compared to MnO. In particular, as the reduction temperature increased, the peaks α and β grew. Oxidized manganese phase appeared to be dominant even after the reduction. The energies of Mn K-edge indicated the presence of Mn(II) species for all Mn-Ni/Al_2O_3 catalysts. As far as XANES was concerned, there was no indication of metallic manganese present in Mn-Ni/Al_2O_3 catalysts.

EXAFS functions weighted with k^3 and their RSFs for Mn-Ni/Al_2O_3 catalysts are displayed in Figures 2 and 3. For Ni K-edge, both EXAFS function and RSF of Mn-Ni/Al_2O_3 were nearly the same as those in Ni foil, in agreement with the results of XANES described above, and the only difference was the magnitudes of spectra. The RSF of Ni K-edge of Mn-Ni/Al_2O_3 coincided with that

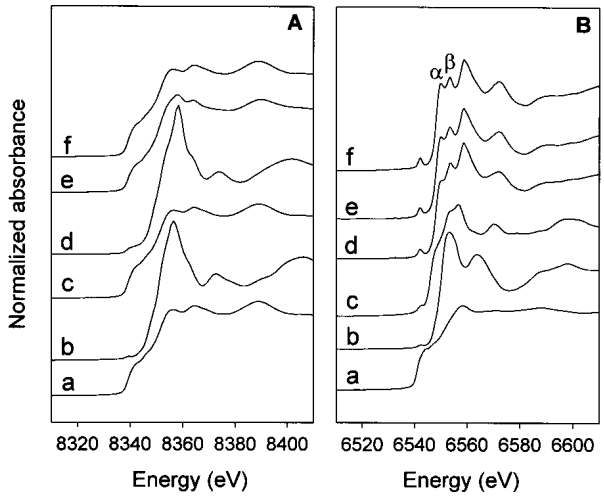

Figure 1
XANES of Ni (A) and Mn (B) K-edges of Mn-Ni/Al_2O_3 catalysts.
A. (a) Ni foil, (b) NiO, (c) Ni/Al_2O_3 reduced at 1073 K, (d) Mn-Ni/Al_2O_3 reduced at 973 K, (e) Mn-Ni/Al_2O_3 reduced at 1073 K, and (f) Mn-Ni/Al_2O_3 reduced at 1173 K.
B. (a) Mn foil, (b) $MnCO_3$, (c) MnO, (d) Mn-Ni/Al_2O_3 reduced at 973 K, (e) Mn-Ni/Al_2O_3 reduced at 1073 K, and (f) Mn-Ni/Al_2O_3 reduced at 1173 K.

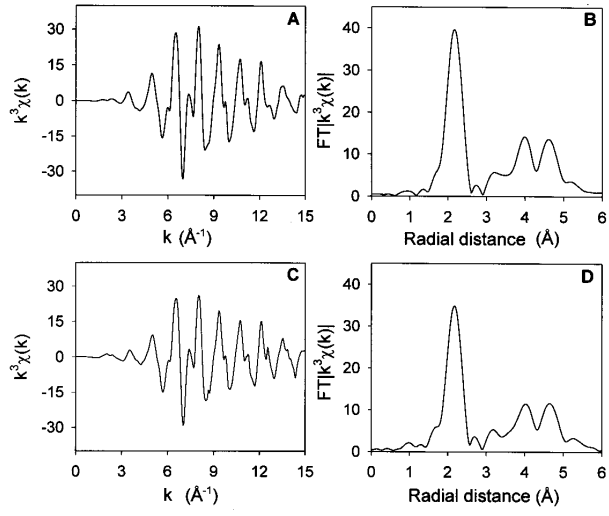

Figure 2
K^3-weighted EXAFS function (A, C) and its Fourier transformation (B, D) at K-edge of Ni foil (A, B) and Mn-Ni/Al_2O_3 catalyst reduced at 1073 K (C, D).

of Ni foil up to the fourth shell. Any contribution from manganese as a nearest neighbour did not appear.

EXAFS curve fitting results confirmed this, as shown in Table 1A. The standard for fitting was a Ni-Ni single scattering synthesized with FEFF code using available structural parameters for Ni metal. An adjustable parameter for the fitting, S_o^2 was fixed to 0.86, which was obtained from the curve fitting of experimental data for nickel foil with the theoretical EXAFS equation. Considering Ni-Mn scattering together with Ni-Ni scattering, did not improve the EXAFS fittings at all.

Table 1
EXAFS fitting results of Ni-Mn/Al_2O_3 catalysts reduced at different temperatures.

A. Ni K-edge

	N_{Ni-Ni}	R_{Ni-Ni} (Å)	σ^2 (Å^2)	ΔE_0 (eV)	R-factor[a]
Ni foil	12.0	2.492	0.00645		
Ni/Al_2O_3 reduced at 1073K	11.1	2.492	0.00630	-2.48	0.00075
Ni-Mn/Al_2O_3 reduced at 1073K	9.9	2.488	0.00619	-1.72	0.00212
Ni-Mn/Al_2O_3 reduced at 1173K	11.7	2.496	0.00637	-3.56	0.00315

B. Mn K-edge

	shell	N	R (Å)	σ^2 (Å^2)	ΔE_0 (eV)	R-factor[a]
Mn-Ni/Al_2O_3 reduced at 973K	Ni	0.05	2.634	-0.0146	-8.28	0.02910
	Al	0.71	3.420	-0.0113		
Mn-Ni/Al_2O_3 reduced at 1073K	Ni	0.70	2.666	0.00016	-5.80	0.00820
	Al	1.65	3.446	-0.00717		
Mn-Ni/Al_2O_3 reduced at 1173K	Ni	2.78	2.714	-0.0165	-2.22	0.01243
	Al	2.40	3.467	-0.0278		

[a]R-factor indicates a sum-of-squares measure of the fractional misfit, which is defined as $R = \sum_{i=1}^{N}\{[\mathrm{Re}(f_i)]^2 + [\mathrm{Im}(f_i)]^2\} / \sum_{i=1}^{N}\{[\mathrm{Re}(\tilde{\chi}_{datai})]^2 + [\mathrm{Im}(\tilde{\chi}_{datai})]^2\}$.

In the case of Mn-Ni/Al_2O_3 catalyst reduced at 973 K, the RSF showed quite a large oxygen contribution, and a small nickel contribution, which was also consistent with XANES result. Thus, the nonlinear EXAFS fitting for this catalyst was not conducted. As seen in Table 1A, irrespective of the presence of manganese, nickel was always metallic. Only difference was the lower Ni-Ni coordination number by 1-3 than that of Ni foil, indicating that large Ni particles were formed.

Unlike Ni K-edge, the EXAFS of Mn K-edge was very complicated. As shown in Figure 3, three distinct peaks appeared in RSF, denoted as α, β, and γ, respectively. The first peak α is due to Mn-O scattering which may originate from manganese oxide, and/or Mn-O scattering in $MnAl_2O_4$, whose formation was confirmed with XRD. As a matter of fact, we have reported previously the formation of MnO phase revealed by XRD in a Mn-Ni/Al_2O_3 catalyst prepared by the incipient wetness impregnation. Although crystalline MnO was not observed with XRD for catalysts prepared by coprecipitation studied here, the formation of X-ray amorphous manganese oxides are highly plausible. The result of XANES described above also suggests the possibility of existence of MnO phase. The peak β can be assigned as Mn-Ni scattering and γ as an Mn-Al scattering of $MnAl_2O_4$. These assignments were confirmed with the results of EXAFS curve fitting summarized in Table 1B. For the fitting of Mn K-edge EXAFS, two standards were employed; Mn-Ni and Mn-Al single scatterings that were also synthesized with the FEFF code using structural parameters of Mn metal and $MnAl_2O_4$. As the reduction temperature increased, both Mn-Ni and Mn-Al coordination numbers increased. This indicates that higher temperatures facilitate the formation of both Mn-Ni bond and $MnAl_2O_4$ phase.

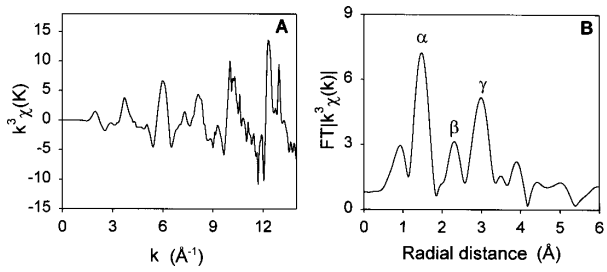

Figure 3
K^3-weighted EXAFS function (A) and its Fourier transformation (B) at Mn K-edge of Mn-Ni/Al_2O_3 catalyst reduced at 1073 K.

Summarizing all results, it can be concluded that Mn-Ni/Al_2O_3 contains large Ni metal particles surrounded by manganese metal and MnO patches. Taking into account very small coordination number of Mn-Ni and no appreciable Ni coordinated with Mn obtained by EXAFS, it appears that manganese metal does not aggregate into a particle but exists as the islands on the large nickel particle ("surface decoration"). Of course, isolated manganese aluminate is also formed in reduced catalysts. Correlated with the catalytic activity of these Mn-Ni/Al_2O_3, such a structure appears to assist the suppression of coke deposition during carbon dioxide reforming of methane. Both manganese metal and manganese oxide islands seem to break large Ni ensembles. Such a partial blockage of nickel surface suppresses the coke deposition because the ensemble size necessary for carbon formation is larger than ensemble size for methane reforming. In addition, there could be other roles of manganese oxide species deposited on the nickel surface. It has been shown that manganese oxide could form a surface carbonate species which reacts with carbon deposited on the surface by methane decomposition (Krylov *et al.*, 1998). Thus, manganese oxide islands in Mn-Ni/Al_2O_3 catalyst may enrich the surface with a reactive carbonate species, which removes the coke deposited on the catalyst surface.

4. Conclusion

XAFS clearly reveals the chemical and structural information of Mn-Ni/Al_2O_3 catalyst used for carbon dioxide reforming of methane. Large nickel metal particle is formed in these catalysts, and the surface of Ni metal is decorated by manganese oxide patch and island-like manganese metal partly. Due to a strong interaction with Al_2O_3 support, manganese aluminate coexists as a separate phase. These structural information suggests the nature of catalytically active species for CO_2 reforming.

References

Ankudinov, A. L., Ravel, B., Rehr, J. J. & Conradson, S. D. (1998). *Phys. Rev. B* **58**(12), 7565-7576.

Chen, Y.-G. & Ren, J. (1994) *Catal. Lett.* **29**, 39-48.

Choi, J.-S., Moon, K.-I., Kim, Y. G., Lee, J. S., Kim, C.-H. & Trimm, D. L. (1998). *Catal. Lett.* **52**, 43-47.

Choi, S. H. & Lee, J. S. (1997). *J. Catal.* **167**, 364-371.

Krylov, O. V., Mamedov, A. Kh., & Mirzabekova, S. R. (1998). *Catal. Today* **42**, 211-215.

Lee, J. S., Choi, S. H., Kim, K. D. & Nomura, M. (1996). *Appl. Catal. B* **7**, 199-212.

Seok, S.-H., Han, S. H., and Lee, J. S. (2000). *Appl. Catal. A*, submitted.

Stern, E. A., Newville, M., Ravel, B., Yacoby, Y. & Haskel, D. (1995) *Physica B* **208&209**, 117-120.